

Staurosporine and Rebeccamycin Aglycones Are Assembled by the Oxidative Action of StaP, StaC, and RebC on Chromopyrrolic Acid

Annaleise R. Howard-Jones and Christopher T. Walsh*

Contribution from the Department of Biological Chemistry and Molecular Pharmacology,
Harvard Medical School, Boston, Massachusetts 02115

Received June 13, 2006; E-mail: christopher_walsh@hms.harvard.edu

Abstract: In the biosynthesis of the antitumor indolocarbazoles rebeccamycin and staurosporine by streptomycetes, assembly of the aglycones involves a complex set of oxidative condensations. Overall formation of aglycones K252c and arcyrflavin A from their biosynthetic precursor chromopyrrolic acid involves four- and eight-electron oxidations, respectively. This process is catalyzed by the remarkable enzyme StaP, with StaC and RebC acting to direct the level of oxidation in the newly formed five-membered ring. An aryl–aryl coupling reaction is integral to this transformation as well as oxidative decarboxylation of the dicarboxypyrrole moiety of chromopyrrolic acid. Herein we describe the heterologous expression of *staP*, *staC*, and *rebC* in *Escherichia coli* and the activity of the corresponding enzymes in constructing the two distinct six-ring scaffolds. StaP is a cytochrome P450 enzyme, requiring dioxygen, ferredoxin, flavodoxin NADP⁺-reductase, and NAD(P)H for activity. StaP on its own converts chromopyrrolic acid into three aglycone products, K252c, arcyrflavin A, and 7-hydroxy-K252c; in the presence of StaC, K252c is the predominant product, while the presence of RebC directs formation of arcyrflavin A. ¹⁸O-Labeling studies indicate that the oxygen(s) of the pyrrolinone and maleimide functionalities of the aglycones formed are all derived from dioxygen. This work allowed for the in vitro reconstitution of the full biosynthetic pathway from L-tryptophan to the staurosporine and rebeccamycin aglycones, K252c and 1,11-dichloroarcyrflavin A.

Introduction

The indolocarbazole antibiotics rebeccamycin and staurosporine (Figure 1) have attracted much attention due to their broad-spectrum antitumor activity. Despite their striking structural similarity, these two compounds exert their biological activity via two distinct pathways. Rebeccamycin and its analogues bearing simple *N*-glycosidic linkages act to stabilize the DNA-topoisomerase I cleavable complex, with a minimum inhibitory concentration of 1.75 μ M.¹ By contrast, staurosporine is one of the strongest known inhibitors of protein kinases, with IC₅₀s in the 1–20 nM range.² Its interaction with the ATP binding pocket of these enzymes explains the ability of staurosporine to interact with most known protein kinases, an activity shared by its bis-linked sugar-indolocarbazole analogues. The presence of the carbohydrate moiety is important for recognition by these cellular targets, as is the planar six-ring scaffold.

Crystal structures have been solved of rebeccamycin analogue SA315F in complex with DNA and human topoisomerase I,³ and of staurosporine in complex with the catalytic subunit of cAMP-dependent protein kinase.⁴ In the case of SA315F, the

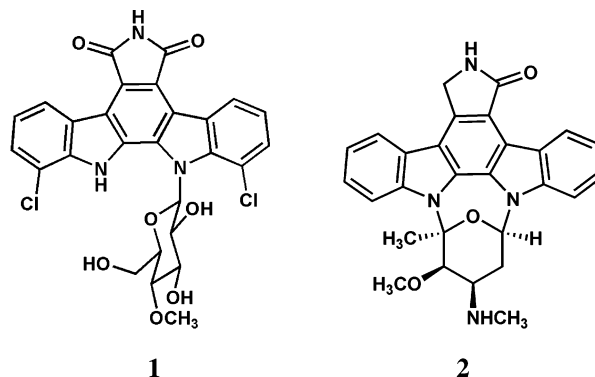
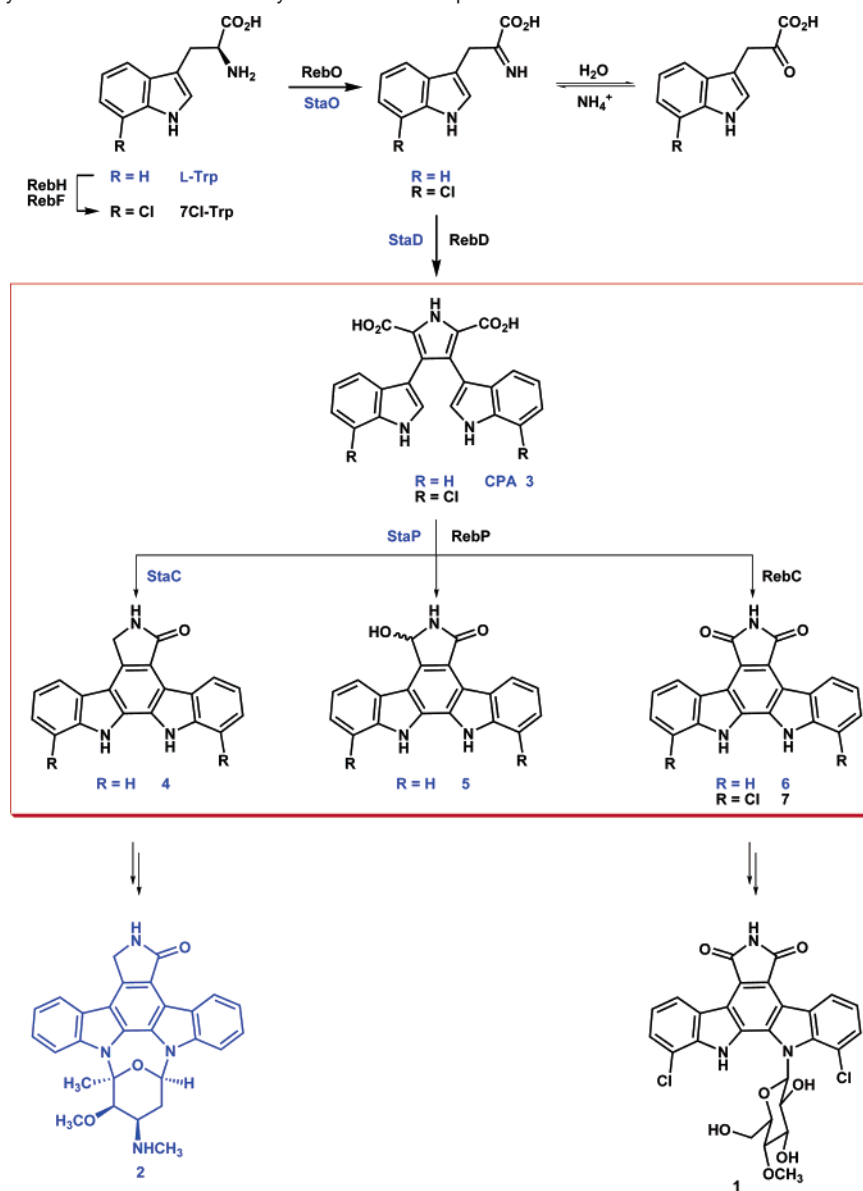


Figure 1. Chemical structures of rebeccamycin 1 and staurosporine 2.

flat scaffold intercalates between the DNA base pairs, and the sugar moiety forms hydrogen bonding interactions in the major groove.³ In the staurosporine–protein kinase structure, the aglycone portion fits snugly into the ATP-binding pocket, roughly superimposing with the position of the purine moiety of ATP, and the indole nitrogens and sugar hydroxyls form key hydrogen-bonding interactions.⁴ These structures clearly demonstrate the importance of the planar, aromatic aglycone core in directing these indolocarbazoles toward their cellular targets.

- (1) Moreau, P.; Anizon, F.; Sancelme, M.; Prudhomme, M.; Bailly, C.; Severe, D.; Riou, J.-F.; Fabbro, D.; Meyer, T.; Aubertin, A.-M. *J. Med. Chem.* **1999**, *42*, 584–592.
- (2) Tamaoki, T.; Nomoto, H.; Takahashi, I.; Kato, Y.; Morimoto, M.; Tomita, F. *Biochem. Biophys. Res. Commun.* **1986**, *135*, 397–402.
- (3) Staker, B. L.; Feese, M. D.; Cushman, M.; Pommier, Y.; Zembower, D.; Stewart, L.; Burgin, A. B. *J. Med. Chem.* **2005**, *48*, 2336–2345.
- (4) Prade, L.; Engh, R. A.; Girod, A.; Kinzel, V.; Huber, R.; Bossemeyer, D. *Structure* **1997**, *5*, 1627–1637.

Scheme 1. Overall Biosynthetic Route to Rebeccamycin 1 and Staurosporine 2

The rebeccamycin and staurosporine indolocarbazole cores are derived from L-tryptophan (L-Trp) via a series of oxidative transformations (Scheme 1). Gene disruption studies combined with isolation of putative intermediates led to an initial description of the biosynthetic pathways to rebeccamycin and staurosporine.^{5–7} Unsurprisingly, the pathways to the two aglycones follow very similar routes, differing only by (1) chlorination at the 7-position of L-Trp en route to rebeccamycin and (2) the oxidation state of the pyrrole-derived five-membered ring, taking the form of a maleimide in rebeccamycin and a pyrrolinone in the staurosporine aglycone. Subsequent *N*-glycosylation and tailoring modifications follow divergent pathways toward rebeccamycin and staurosporine.

In vitro reconstitution and analysis of the biosynthetic enzymes involved in rebeccamycin and staurosporine formation

is only now emerging. Halogenation of L-Trp by RebH (and its flavin reductase partner protein RebF) has been demonstrated⁸ and shown to involve formation of HOCl in the active site.⁹ The formation of chromopyrrolic acid (CPA), a key biosynthetic intermediate, through the joint action of RebO, an L-amino acid oxidase,¹⁰ and RebD (or StaD), a heme-containing oxidase, has also been investigated^{11–13} and shown to proceed via the condensation of two molecules of indole-3-pyruvic acid imine.¹¹ Most recently, in vivo studies of the *N*-glycosyltransferase RebG¹⁴ and in vitro characterization of RebM, the methyl-

- (5) Sánchez, C.; Butovich, I. A.; Braña, A. F.; Rohr, J.; Méndez, C.; Salas, J. A. *Chem. Biol.* **2002**, *9*, 519–531.
 (6) Onaka, H.; Taniguchi, S.-I.; Igarashi, Y.; Furumai, T. *J. Antibiot.* **2002**, *55*, 1063–1071.
 (7) Onaka, H.; Taniguchi, S.-I.; Igarashi, Y.; Furumai, T. *Biosci. Biotechnol. Biochem.* **2003**, *67*, 127–138.

- (8) Yeh, E.; Garneau, S.; Walsh, C. T. *Proc. Natl. Acad. Sci. U.S.A.* **2005**, *102*, 3960–3965.
 (9) Yeh, E.; Cole, L. J.; Barr, E. W.; Bollinger, J. M., Jr.; Ballou, D. P.; Walsh, C. T. *Biochemistry* **2006**, *45*, 7904–7912.
 (10) Nishizawa, T.; Aldrich, C. C.; Sherman, D. H. *J. Bacteriol.* **2005**, *187*, 2084–2092.
 (11) Howard-Jones, A. R.; Walsh, C. T. *Biochemistry* **2005**, *44*, 15652–15663.
 (12) Nishizawa, T.; Grischow, S.; Jayamaha, D.-H. E.; Nishizawa-Harada, C.; Sherman, D. H. *J. Am. Chem. Soc.* **2005**, *128*, 724–725.
 (13) Asamizu, S.; Kato, Y.; Igarashi, Y.; Furumai, T.; Onaka, H. *Tetrahedron Lett.* **2006**, *47*, 473–475.
 (14) Zhang, C.; Albermann, C.; Fu, X.; Peters, N. R.; Chisholm, J. D.; Zhang, G.; Gilbert, E. J.; Wang, P. G.; Van Vranken, D. L.; Thorson, J. S. *Chem. BioChem.* **2006**, *7*, 795–804.

transferase that catalyzes the final step in rebeccamycin biosynthesis, were reported.^{14,15}

To date, no biochemical studies on the enzymes involved in aglycone ring construction, StaP and StaC (or RebP and RebC), have been reported. Gene knockouts of *rebC* produced three distinct aglycone products, 1,11-dichloro-K252c, 1,11-dichloro-7-hydroxy-K252c, and 1,11-dichloroarcyriaflavin A 7.⁷ Similarly, constructs bearing *rebO*, *rebD*, and *rebP* (or *staP*) resulted in the formation of three products—K252c 4, 7-hydroxy-K252c 5, and arcyriaflavin A 6—while the additional presence of *staC* or *rebC* led to exclusive formation of K252c 4 or arcyriaflavin A 6, respectively (Scheme 1).¹⁶

RebP and StaP have been annotated as cytochrome P450 enzymes and display the appropriate signature motifs, including a (FXXGXHXGXG) motif bearing the putative axial cysteine for heme-iron ligation. RebC and StaC have been annotated as flavin adenine dinucleotide (FAD) monooxygenases and contain the characteristic (GXGXXG) motif of the Rossman $\beta\alpha\beta$ dinucleotide binding fold,¹⁷ as well as the GD motif believed to be important for hydrogen bonding to the 3'-hydroxyl of the FAD ribosyl moiety.¹⁸ The RebP and StaP proteins share 54% identity at the amino acid level, and RebC and StaC are 65% identical. Previous work on enzymes from the *reb* and *sta* systems—namely, RebO, RebD, and RebG—has shown that they are relatively promiscuous in terms of accepting substrates from the alternative (Sta) system.^{10,11,14}

The overall reaction catalyzed by StaP is intriguing as it involves both aryl–aryl coupling and double oxidative decarboxylation to facilitate net four- to eight-electron oxidation. While aryl–aryl coupling reactions are not uncommon in biosynthetic pathways, few enzymes mediating such steps have been examined in biochemical detail.^{19–21} The opportunity to study this class of enzymatic reactions, as well as the intriguing oxidative decarboxylation process, lent the StaP/StaC (and RebP/RebC) system much appeal as a focus of biosynthetic and mechanistic investigations.

Experimental Section

Amino acids, spinach ferredoxin, and other general reagents were purchased from Sigma-Aldrich; (¹⁸O)-labeled water was obtained from Cambridge Isotope Laboratories; and (¹⁸O)-labeled oxygen was purchased from Chemgas. CPA was prepared as previously described.¹¹ *E. coli* flavodoxin NADP⁺-reductase was overproduced and purified (construct kindly provided by Prof. Rowena Matthews), giving 10 mg protein per liter culture. *E. coli* TOP10 and BL21(DE3) cells were obtained from Invitrogen. pET28a and pET22b plasmids were purchased from Novagen. Restriction enzymes were obtained from New England Biolabs. Nickel–nitrilotriacetic acid–agarose (Ni-NTA) gel was obtained from QIAGEN. The HiLoad 26/60 Superdex 200 column used was obtained from GE Healthcare. Electrospray mass spectra were collected by liquid chromatography–mass spectrometry (LCMS), using a Shimadzu LCMS-QP8000α equipped with a Higgins Analytical (Mountain View, CA) Sprite Targa C18 column (20 × 2.1 mm) running

at 0.5 mL·min⁻¹ [0 → 100% acetonitrile in water, with 0.1% formic acid] in positive ion mode. NMR spectra were recorded on a Varian 600 MHz Fourier Transform NMR spectrometer. UV/visible spectra were collected on a Cary 50 Bio UV–visible spectrophotometer. DNA sequencing was performed by the Biopolymers Facility, Department of Genetics, Harvard Medical School, Boston, and by the Molecular Biology Core Facility, Dana-Farber Cancer Institute, Boston. Chemical ionization mass spectrometry was performed by the Mass Spectrometry Service, Department of Chemistry and Chemical Biology, Harvard University, Boston.

DNA Isolation and Manipulation. *Lechevalieria aerocolonigenes* (ATCC 39243) and *Streptomyces longisporoflavus* (DSM 10189) were grown in yeast-malt extract medium (3 g·L⁻¹ yeast extract; 5 g·L⁻¹ malt extract; pH 7.0) for preparation of chromosomal genomic DNA. The cultures were incubated at 26 °C and 250 rpm for 18 h prior to isolation of genomic DNA. Standard methods for DNA isolation and manipulation were performed as described by Sambrook et al.²² DNA fragments were isolated from agarose gels using a QIAGEN gel extraction kit.

Cloning, Expression, and Purification of StaP, StaC, and RebC. Primers for *staP* (5'-GGAGAGCATATGCCATCCGCGAC-GCTGC-3' and 5'-GTCAAGCTTGGGGTGGCTGGCCGAGGG-3'), *staC* (5'-GGAGAGCATATGACGCATTCGGGTGAGCGGACC-3' and 5'-GTCAAGCTTGGCCCCGGGCTACGGGGCGCGGC-3') and *rebC* (5'-GGAGAGCATATGAACGCGCCCATCGAA-3' and 5'-GTCAAGCTTTCACGCGGCACCCCTCAC-3') contained *NdeI* and *HindIII* sites (italicized) and were used to amplify the relevant genes of interest. These orfs were cloned into the corresponding *NdeI/HindIII* sites of pET28a (*rebC*) and pET22b (*staP* and *staC*). The sequences of the cloned expression vectors were confirmed by DNA sequencing. Some disparities were observed with the published sequences of *S. longisporoflavus staP* and *staC*;²³ these are described in Supporting Information and have been deposited at GenBank under accession numbers DQ861904 and DQ861905, respectively.

E. coli BL21(DE3) cells overexpressing *staP* were grown in Luria–Bertani medium supplemented with ampicillin (100 μg·mL⁻¹). After 22 h growth at 15 °C, OD₆₀₀ = 0.4 was reached, at which point δ-aminolevulinic acid (1 mM) and ferrous ammonium sulfate (32 mM) were added. The cells were induced with 100 μM isopropyl β-D-thiogalactoside (IPTG) and grown for a further 14 h at 15 °C. *E. coli* BL21(DE3) cells overexpressing *staC* were grown in Luria–Bertani medium supplemented with ampicillin (100 μg·mL⁻¹). Cells were grown at 15 °C to OD₆₀₀ = 0.5 and then induced with 100 μM IPTG and grown for a further 72 h at 15 °C. *E. coli* BL21(DE3) cells overexpressing *rebC* were grown in Luria–Bertani medium supplemented with kanamycin (50 g·mL⁻¹). Cells were grown at 15 °C to OD₆₀₀ = 0.4 and then induced with 100 μM IPTG and grown for a further 72 h at 15 °C.

Cells were harvested by centrifugation (20 min at 3000g) and resuspended in 20 mM Tris-HCl (pH 8.0), 300 mM NaCl, 5 mM imidazole. Resuspended cells were lysed (2 passes at 10000–15000 psi, Avestin EmulsiFlex-C5 high-pressure homogenizer), and the cell debris was removed by centrifugation (35 min at 95000g).

C-His₆-tagged-StaP, C-His₆-tagged-StaC, and N-His₆-tagged-RebC were purified by Ni-NTA affinity chromatography. Eluted protein fractions were purified further by passage through a HiLoad 26/60 Superdex 200 gel filtration column; fractions containing the protein of interest were collected and combined. (RebC could be reconstituted with FAD to 55% occupancy by incubating with 10 equiv of FAD at 4 °C for 2 h prior to gel filtration; however, the sample prior to reconstitution (with 33% FAD) showed higher activity and was used

(15) Zhang, C.; Weller, R. L.; Thorson, J. S.; Rajski, S. R. *J. Am. Chem. Soc.* **2006**, *128*, 2760–2761.

(16) Sánchez, C.; Zhu, L.; Braña, A. F.; Salas, A. P.; Rohrer, J.; Méndez, C.; Salas, J. A. *Proc. Natl. Acad. Sci. U.S.A.* **2005**, *102*, 461–466.

(17) Rossman, M. G.; Moras, D.; Olsen, K. W. *Nature* **1974**, *250*, 194–199.

(18) Eppink, M. H. M.; Schreuder, H. A.; Van Berkel, W. J. H. *Protein Sci.* **1997**, *6*, 2454–2458.

(19) Funai, N.; Funabashi, M.; Ohnishi, Y.; Horinouchi, S. *J. Bacteriol.* **2005**, *187*, 8149–8155.

(20) Zhao, B.; et al. *J. Biol. Chem.* **2005**, *280*, 11599–11607.

(21) Zerbe, K.; Woithe, K.; Li, D. B.; Vitali, F.; Bigler, L.; Robinson, J. A. *Angew. Chem., Int. Ed.* **2004**, *43*, 6709–6713.

(22) Sambrook, J.; Russell, D. W. *Molecular cloning: a laboratory manual*, 3rd ed.; Cold Spring Harbor Laboratory Press: Cold Spring Harbor, NY, 2000.

(23) Schupp, T.; Engel, N.; Bietenhader, J.; Toupet, C.; Pospiech, A. U.S. Pat. 6,210,935; 2001.

for activity assays.) The proteins were flash-frozen in liquid nitrogen and stored in 25 mM HEPES, pH 7.5, 10% glycerol (with 150 mM NaCl, in the case of StaC and RebC) at -80°C . Protein concentrations were determined using the method of Bradford, with bovine serum albumin (BSA) as a standard.²⁴ The total yield of protein was $3\text{ mg}\cdot\text{L}^{-1}$ culture for C-His₆-StaP, $11\text{ mg}\cdot\text{L}^{-1}$ culture for C-His₆-StaC and $18\text{ mg}\cdot\text{L}^{-1}$ for N-His₆-RebC.

Biochemical Characterization of StaP, StaC, and RebC. The molecular masses of the proteins were determined by gel filtration, using known standards (Sigma-Aldrich) as reference. To determine the reduced carbon monoxide difference spectrum of StaP, sodium dithionite was added (to a final concentration of 1 mM) to an anaerobic cuvette containing StaP (21 μM), after which CO (g) was bubbled through the solution for 5 min. UV/visible spectra (200–800 nm) were taken before and after this procedure, and the difference spectrum calculated. The binding curve of CPA for StaP was determined by measuring a difference UV/visible absorption spectrum following addition of varying quantities of CPA to a solution containing 37 μM StaP in 75 mM HEPES, pH 7.5 (difference spectra measured relative to solution with no CPA). The difference absorbance value at 423 nm was subtracted from the value at 388 nm, and the resulting parameter (dA) was plotted against CPA concentration to obtain the K_D for CPA.

The RebC cofactor was identified as FAD by HPLC and UV/visible spectroscopy. A sample of protein was denatured (100°C , 30 min) and the supernatant analyzed by HPLC, with comparison to standard samples of FAD and flavin mononucleotide (FMN). The FAD content of the protein was determined using the known extinction coefficient for FAD (ϵ_{450} $11\,300\text{ M}^{-1}\cdot\text{cm}^{-1}$). Apo-RebC was prepared using the His-tag immobilization method of Hefti et al.²⁵

The reduced β -nicotinamide adenine dinucleotide 2'-phosphate (NADPH) and NADH oxidase activity of RebC and StaC (10 μM) were determined by following the consumption of NADPH (or NADH) (200 μM initial concentration) over time in the presence of FAD in 75 mM HEPPS, pH 8.0. NAD(P)H kinetic parameters were determined at 400 μM FAD; K_m values for FAD were determined at 200 μM NADH. NADPH and NADH consumption rates were calculated using A_{340} values, with reference to a standard curve, and corrected for background air oxidation of NADPH or NADH. Reaction progress was accompanied by an appropriate decrease in the absorbance at 450 nm, consistent with the reduction of FAD to FADH₂.

Biochemical StaP/StaC Pull-Down Experiments. To facilitate co-transformation into *E. coli* BL21(DE3) cells and pull-down experiments, the *staP* and *staC* genes were subcloned into pRSF-1b (as N-terminal His₆-tagged constructs) and into pET22b (as untagged constructs). Thus, *staP* and *staC* were subcloned from pET28a into pRSF-1b using *NcoI* and *HindIII* restriction sites, and from pET28a into pET22b using *NdeI* and *HindIII* sites. NHis-*staP*-pRSF-1b and *staC*-pET22b were co-transformed into *E. coli* BL21(DE3) cells; NHis-*staC*-pRSF-1b and *staP*-pET22b were co-transformed similarly. The resulting *E. coli* BL21(DE3) cells overproducing NHis-StaP/StaC or NHis-StaC/StaP (2 L each) were grown in Luria–Bertani broth supplemented with δ -aminolevulinic acid (1 mM), ferrous ammonium sulfate (40 μM), ampicillin (100 $\mu\text{g}\cdot\text{mL}^{-1}$), and kanamycin (50 $\mu\text{g}\cdot\text{mL}^{-1}$). After 17 h, cultures reached $\text{OD}_{600} = 0.7$, at which point they were induced with 60 μM IPTG. Growth was continued for a further 28 h at 15°C . Cells were harvested and lysed and the debris pelleted as described above. The lysate was loaded on pre-equilibrated Ni-NTA resin and eluted with increasing concentrations of imidazole (5 to 200 mM) in 20 mM Tris, pH 8, 300 mM NaCl.

HPLC Activity Assays. Conversion of CPA 3 to aglycones 4, 5, and/or 6 was examined by analytical reversed phase HPLC. A typical assay examined the turnover of 150 μM CPA by StaP (1 μM) and StaC (5 μM) or RebC (5 μM), in the presence of BSA (1 $\text{mg}\cdot\text{mL}^{-1}$),

spinach ferredoxin (20 μM), *E. coli* flavodoxin NADP⁺-reductase (1 μM), and NAD(P)H (5 mM) in 75 mM HEPPS buffer, pH 8.0. Reactions were quenched by addition of methanol (2 volumes), and the protein was removed by centrifugation. HPLC assays were run on a Beckman System Gold (Beckman Coulter) with a Vydac C18 column (250 \times 10 mm) at $1\text{ mL}\cdot\text{min}^{-1}$ or a Higgins analytical C18 column (50 \times 4.6 mm) at $3\text{ mL}\cdot\text{min}^{-1}$ using a gradient of 0 \rightarrow 60% acetonitrile in 0.1% trifluoroacetic acid (TFA). The elution profiles were monitored at 280, 289, or 315 nm.

Anaerobic Experiments. Anaerobic assays were performed in a Unilab glovebox (Mbraun, Stratham, NH), with oxygen levels maintained at or below 2 ppm. All reagents and solutions were degassed by bubbling argon for 10 min prior to their introduction into the glovebox, then equilibrated overnight to remove residual traces of oxygen. Incubations were quenched immediately prior to removal from the glovebox by addition of two volumes of methanol.

¹⁸O-Incorporation Experiments. ¹⁸O-Incorporation studies were used to determine the origin of the oxygen atom(s) in the aglycone products. CPA (150 μM) was incubated with StaP (1 μM), StaC or RebC (5 μM), ferredoxin (20 μM), flavodoxin NADP⁺-reductase (1 μM), NADPH (5 mM), and BSA (1 $\text{mg}\cdot\text{mL}^{-1}$) in 75 mM HEPPS, pH 8.0 (50 μL), for 15 h in the presence of either ¹⁸O-labeled dioxygen or ¹⁸O-labeled water. After quenching with methanol (2 volumes), the supernatant was purified by HPLC, and the peaks corresponding to the relevant aglycone products were collected and analyzed by electrospray mass spectrometry (positive ion mode).

In Vitro Reconstitution of Complete Pathway to the Rebecca-mycin Aglycone 1,11-Dichloroarcyriaflavin A 7. 7-Chloro-L-tryptophan (5 mM) was incubated with ReBO (1 μM), RebD (3 μM), StaP (1 μM), and RebC (5 μM) in the presence of NADH (5 mM), ferredoxin (20 μM), flavodoxin NADP⁺-reductase (1 μM), and BSA (1 $\text{mg}\cdot\text{mL}^{-1}$) in HEPES, pH 7.5, at room temperature for 46 h, with further addition of NADH (10 mM), ferredoxin (20 μM), flavodoxin NADP⁺-reductase (1 μM), StaP (1 μM), and RebC (5 μM) after 22 h and additional NADH (10 mM) at 25 h. The product 7 was purified by reversed phase HPLC and analyzed by chemical ionization mass spectrometry (positive ion mode). The compound is observed by mass spectrometry as the (ring opened) maleamic acid form, its isotope pattern consistent with that of 1,11-dichloroarcyriaflavin A 7: m/z [M + H]⁺ 412 (97%), 413 (22%), 414 (100%), 415 (20%).

Synthesis of Aglycone Standards, Arcyriaflavin A 6, and 7-Hydroxy-K252c 5. Arcyriaflavin A 6 was synthesized from arcyrirubin A 9 by palladium(II)-mediated aryl–aryl coupling, according to the method of Harris et al.,²⁶ to give a yellow solid with spectral properties consistent with those in the literature.²⁷ ¹H NMR (600 MHz, *d*₆-acetone) δ 11.10 (br s, 2H, H₁₂ and H₁₃), 9.79 (br s, 1H, H₆), 9.16 (d, 2H, *J* 7.5 Hz, H₄ and H₈), 7.72 (d, 2H, *J* 8.0 Hz, H₁ and H₁₁), 7.55 (t, 2H, *J* 7.5 Hz, H₂ and H₁₀), 7.37 (t, 2H, *J* 7.5 Hz, H₃ and H₉) ppm; m/z (ES⁺) 326 [M + H]⁺.

The synthesis of 7-hydroxy-K252c 5 was achieved by lithium aluminum hydride-mediated reduction of arcyriaflavin A 6, as described in the literature.²⁶ ¹H NMR (600 MHz, *d*₆-acetone) δ 10.91, 10.77 (2 \times br s, 2H, H₁₂ and H₁₃), 9.33 (d, 1H, *J* 7.9 Hz, 1 of H₄ or H₈), 8.50 (d, 1H, *J* 7.9 Hz, 1 of H₄ or H₈), 7.76 (br s, 1H, H₆), 7.68 (d, 1H, *J* 8.3 Hz, 1 of H₁ or H₁₁), 7.63 (d, 1H, *J* 8.2 Hz, 1 of H₁ or H₁₁), 7.46 (t, 1H, *J* 7.6 Hz, 1 of H₂ or H₁₀), 7.43 (t, 1H, *J* 7.6 Hz, 1 of H₂ or H₁₀), 7.31 (t, 1H, *J* 7.3 Hz, 1 of H₃ or H₉), 7.27 (t, 1H, *J* 7.2 Hz, 1 of H₃ or H₉), 6.58 (s, 1H, H₇), 5.27 (br s, 1H, 7-OH) ppm; m/z (ES⁺) 328 [M + H]⁺.

Results

Purification and Characterization of StaP, StaC, and RebC. StaP was overproduced and purified as a C-terminal His₆-

(24) Bradford, M. M. *Anal. Biochem.* **1976**, *72*, 248–254.

(25) Hefti, M. H.; Milder, F. J.; Boeren, S.; Vervoort, J.; Van Berkel, W. J. H. *Biochim. Biophys. Acta* **2003**, *1619*, 139–143.

(26) Harris, W.; Hill, C. H.; Keech, E.; Malsher, P. *Tetrahedron Lett.* **1993**, *34*, 8361–8364.

(27) Bergman, J.; Pelcman, B. *J. Org. Chem.* **1989**, *54*, 824–828.

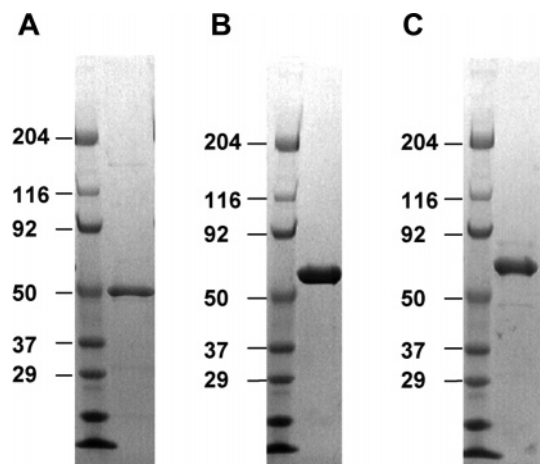


Figure 2. SDS-PAGE gel of (A) StaP (48 kDa); (B) RebC (59 kDa); and (C) StaC (61 kDa).

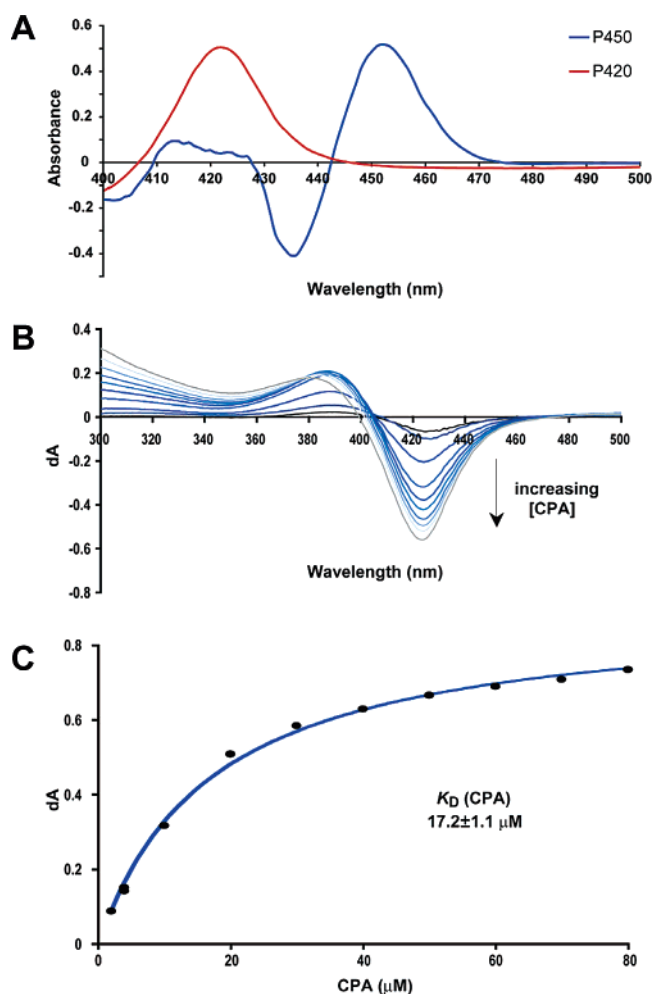


Figure 3. (A) Reduced carbon monoxide binding spectrum of StaP in active (blue) and inactive (red) forms; (B) type I substrate binding curve; and (C) dissociation curve for interaction of CPA with StaP.

tagged protein of molecular mass 48 kDa ($3 \text{ mg} \cdot \text{L}^{-1}$ culture) (Figure 2A). The protein displayed the typical reduced carbon monoxide difference spectrum of a cytochrome P450, in contrast to alternative (inactive) preparations of the enzyme, which gave the P420 form (Figure 3A). A type I binding spectrum was observed on interaction with its putative substrate CPA (Figure 3B), with a K_D of $17.2 \pm 1.1 \mu\text{M}$ (Figure 3C).

RebC was overproduced and purified at $18 \text{ mg} \cdot \text{L}^{-1}$ culture as an N-terminal His₆-tagged 59 kDa protein (Figure 2B). It contained 33% bound FAD on isolation and could be reconstituted to 55% bound FAD, though the protein as isolated (with 33% FAD) was used in activity assays due to improved turnover at this level of FAD incorporation, as discussed below. StaC was overproduced and purified as a C-terminal His₆-tagged 61 kDa protein at $11 \text{ mg} \cdot \text{L}^{-1}$ culture (Figure 2C). It contained no bound cofactors and could not be reconstituted with FAD. RebC ran predominantly as a monomer on gel filtration, whereas StaC showed the elution profile of a monomer/dimer mixture, with the dimer being the predominant oligomeric state.

The kinetic profile of StaC and RebC in oxidizing NAD(P)H in the presence of FAD and FMN was examined. No activity was observed in the presence of FMN or, in the case of RebC, in the presence of FAD and NADPH. Saturation could not be achieved under the assay conditions for the StaC-induced turnover of NAD(P)H and FAD due to high K_m values for NAD(P)H and the saturation limits of the detector; k_{cat}/K_m values were extracted by linear regression analysis of the line generated by a plot of velocity versus NAD(P)H concentration. StaC displayed a k_{cat}/K_m of $30 \pm 3 \text{ mM}^{-1} \text{ min}^{-1}$ with NADH and $2.3 \pm 0.2 \text{ mM}^{-1} \text{ min}^{-1}$ with NADPH; in the case of RebC, kinetic parameters could only be extracted for NADH oxidase activity (k_{cat} $8.3 \pm 1.4 \text{ min}^{-1}$; K_m $138 \pm 58 \mu\text{M}$; k_{cat}/K_m $60 \pm 27 \text{ mM}^{-1} \text{ min}^{-1}$). NADH is thus the preferred reductant for StaC- and RebC-mediated turnover of FAD.

As saturation of NADH could not be examined under these assay conditions, an apparent K_m for FAD was calculated at $200 \mu\text{M}$ NADH. The K_m (apparent) for FAD was $140 \pm 30 \mu\text{M}$ for StaC and $70 \pm 20 \mu\text{M}$ for RebC. The relatively high K_m values for FAD are not surprising given the low observed binding affinity for FAD (especially in the case of StaC). Nonetheless, these data collectively suggest that RebC and StaC are capable of reducing FAD in situ and may therefore function as flavin- dependent monooxygenases.

To investigate the possibility of complex formation between StaP and StaC, biochemical pull-down experiments were conducted using cells overproducing both StaP and StaC simultaneously, one as a His₆-tagged construct and the other as an untagged protein. These studies showed no evidence for a stable complex between StaP and StaC. The His₆-tagged protein bound to Ni-NTA resin and required high imidazole concentrations for its elution, while its untagged partner eluted in the initial flow-through.

Aglycone Formation by StaP, StaC, and RebC. The catalytic cycle of a cytochrome P450 typically involves the four-electron reduction of dioxygen to water coupled to a two-electron substrate oxidation, the additional two electrons coming from an external redox partner system. The most commonly observed redox partner system for cytosolic prokaryotic P450s is a two-component ferredoxin/ferredoxin reductase (or flavodoxin/flavodoxin reductase) system; eukaryotic P450s are often membrane-bound proteins that interact with a membrane-bound cytochrome P450 reductase.²⁸ NAD(P)H is the ultimate electron source for both of these systems. As StaP displayed all of the characteristic traits of a cytochrome P450 enzyme, a

(28) McLean, K. J.; Sabri, M.; Marshall, K. R.; Lawson, R. J.; Lewis, D. G.; Clift, D.; Balding, P. R.; Dunford, A. J.; Warman, A. J.; McVey, J. P.; Quinn, A. -M.; Sutcliffe, M. J.; Scrutton, N. S.; Munro, A. W. *Biochem. Soc. Trans.* **2005**, *33*, 796–801.

ferredoxin/flavodoxin NADP⁺ reductase system was investigated as the potential redox partner for this enzymatic reaction.

Indeed, incubation of StaP with CPA, NADH (or NADPH), spinach ferredoxin, and *E. coli* flavodoxin NADP⁺-reductase under aerobic conditions led to the formation of several products (Figure 4A), the major three coeluting with authentic standards for compounds **4**, **5**, and **6**. These were formed in an approximately 1:7:1 ratio. The identities of these products were further confirmed by comparison of the UV/visible absorbance spectra and mass spectra with authentic materials. The inclusion of StaC in this reaction mixture led primarily to the formation of K252c **4**; the presence of RebC gave predominantly arcyriflavin A **6**. Incubation of CPA with StaC (or RebC), NAD(P)H, ferredoxin, and flavodoxin NADP⁺-reductase in the absence of StaP gave no observable turnover; similarly, omission of NAD(P)H, ferredoxin, or flavodoxin NADP⁺-reductase from the StaP/StaC reaction mixture prevented the formation of any aglycone products. Spinach ferredoxin NADP⁺-reductase (Sigma) was also able to reduce spinach ferredoxin and hence facilitate the StaP-mediated reaction, however due to supply difficulties, *E. coli* flavodoxin NADP⁺-reductase was used instead. Cytochrome P450 reductase could not substitute for the ferredoxin/flavodoxin NADP⁺-reductase system. The reaction was optimized in terms of pH, NAD(P)H, ferredoxin, and flavodoxin NADP⁺-reductase concentrations and StaP:StaC (or StaP:RebC) ratio.

The assay was also carried out under anaerobic conditions to assess the oxygen-dependence of this reaction. Aglycone **4** was formed on introduction of oxygen (Figure 4B, +O₂ trace), as previously discussed, but no aglycone formation was observed under anaerobic conditions (Figure 4B, -O₂ trace). New peaks were observed to form that were not seen in aerobic incubation mixtures; however, these were also formed in control anaerobic incubations of ferredoxin and flavodoxin NADP⁺-reductase in HEPPS buffer (Figure 4B). These peaks therefore arise independently of any interaction with CPA, StaP, or StaC.

In addition to the turnover of CPA to aglycones **4**, **5**, and **6**, the complete reconstitution of the biosynthetic pathway from 7-chloro-L-tryptophan (7-Cl-L-Trp) to the rebeccamycin aglycone 1,11-dichloroarcyriflavin A **7** was also demonstrated. Thus, incubation of 7-Cl-L-Trp with RebO, RebD,¹¹ StaP, and RebC, along with NADH, ferredoxin, and flavodoxin NADP⁺-reductase, resulted in the formation of 1,11-dichloroarcyriflavin A **7**. This result demonstrates the ability of StaP to accept the 1,11-dichloro-CPA analogue, produced as an intermediate in this assay by the action of RebO and RebD. Similar promiscuity has also been observed in the behavior of earlier enzymes in the rebeccamycin and staurosporine clusters.^{10–12}

Dependence of Reaction Rate on FAD. The StaP/StaC and StaP/RebC reactions showed complex biphasic behavior with respect to their dependence on FAD concentration (Figure 5). While exogenous FAD was not required for the StaP/StaC reaction, a 3.6-fold enhancement of *k*_{cat} was observed on inclusion of 0.5 μM FAD (0.1 equiv per StaC) in the reaction mixture. As FAD concentrations were increased beyond this level, an inhibitory effect was observed, with the rate at 10 μM FAD dropping more than 6.5-fold relative to the rate observed in the absence of FAD. FAD gave a similar inhibition profile in the reaction of StaP and RebC with CPA, the optimal FAD concentration being at 0.33 equiv per RebC molecule. This ratio corresponds to the FAD content isolated in the native protein.

A control assay omitting StaC and RebC from the reaction showed no difference in rate between 0 and 0.5 μM FAD, but significant rate suppression at 10 μM FAD (data not shown). A 20-fold increase in flavodoxin NADP⁺-reductase concentration restored 40% of the activity lost due to the increase in FAD concentration to 10 μM; increases in ferredoxin concentration gave no such rate enhancement (data not shown). This indicates that the rate enhancement at low FAD concentrations (up to 0.5 μM) is probably due to interaction of FAD with StaC (or RebC), whereas the inhibitory effect of FAD at high concentrations is likely due to a flavodoxin NADP⁺-reductase dependent effect. We postulate that this may be due to reduction of FAD in solution by the reductase or due to equilibration of internally generated FADH₂ in the flavodoxin NADP⁺-reductase active site with free FAD in solution. Therefore the optimal FAD concentration for this assay betrays a fine balance between competing components of the redox system involved in this reaction.

Attempted Turnover of Possible Biosynthetic Intermediates. In order to probe the overall reaction pathway, we investigated the ability of the StaP/StaC and StaP/RebC systems to turn over possible biosynthetic intermediates to the final aglycone products. Incubation of arcyriflavin A **9** with RebC and/or StaP under the previously described conditions gave no observable formation of aglycones **4**, **5**, or **6** (Figure 4C-i). Similarly, incubation of K252c **4** or 7-hydroxy-K252c **5** with StaP and/or RebC gave no formation of any other aglycone products (Figure 4C-ii and -iii). Incubation of arcyriflavin A **6** with StaC and/or StaP gave no conversion to K252c **4** or 7-hydroxy-K252c **5** (Figure 4C-iv). Thus it seems that arcyriflavin A **9** is not a biosynthetic intermediate in the conversion of CPA to aglycones **4**, **5**, and **6**. Furthermore, aglycones **4**, **5**, and **6** are not interconvertible, but appear to diverge from a common biosynthetic intermediate.

¹⁸O-Incorporation Experiments. Incubations of CPA with StaP/StaC and StaP/RebC were conducted in the presence of ¹⁸O-labeled dioxygen or ¹⁸O-labeled water to determine the origin of the oxygen atoms in K252c **4** and arcyriflavin A **6**. The mass spectra of the aglycone products thus obtained were determined, demonstrating that the amide oxygen of K252c **4** and both oxygens of arcyriflavin A **6** are derived from dioxygen (Figure 6).

Incubation of CPA with StaP and StaC in the presence of ¹⁸O-labeled water and unlabelled dioxygen gave a product with *m/z* 312, identical to the standard K252c **4**. To the contrary, incubation in the presence of unlabelled water and ¹⁸O-labeled dioxygen led to an increase of two mass units in the K252c product obtained. This mass shift is consistent with the incorporation of oxygen from ¹⁸O-dioxygen into K252c **4**.

Similar assays were conducted with CPA in the presence of StaP and RebC to look for oxygen-18 incorporation into arcyriflavin A **6**. Product **6** obtained on incubation with unlabelled oxygen gave *m/z* 326, as seen for the native product. Incubation with ¹⁸O-labeled dioxygen and unlabelled water gave a mass shift of +4 (*m/z* 330), in accord with the incorporation of two molecules of ¹⁸O from the labeled dioxygen. Thus it seems that the two maleimide oxygens of **6** and the one amide oxygen of **4** are directly derived from dioxygen.

Steady-State Kinetic Studies of StaP/StaC and StaP/RebC Turnover. The kinetics of formation of aglycones **4** and **6** by

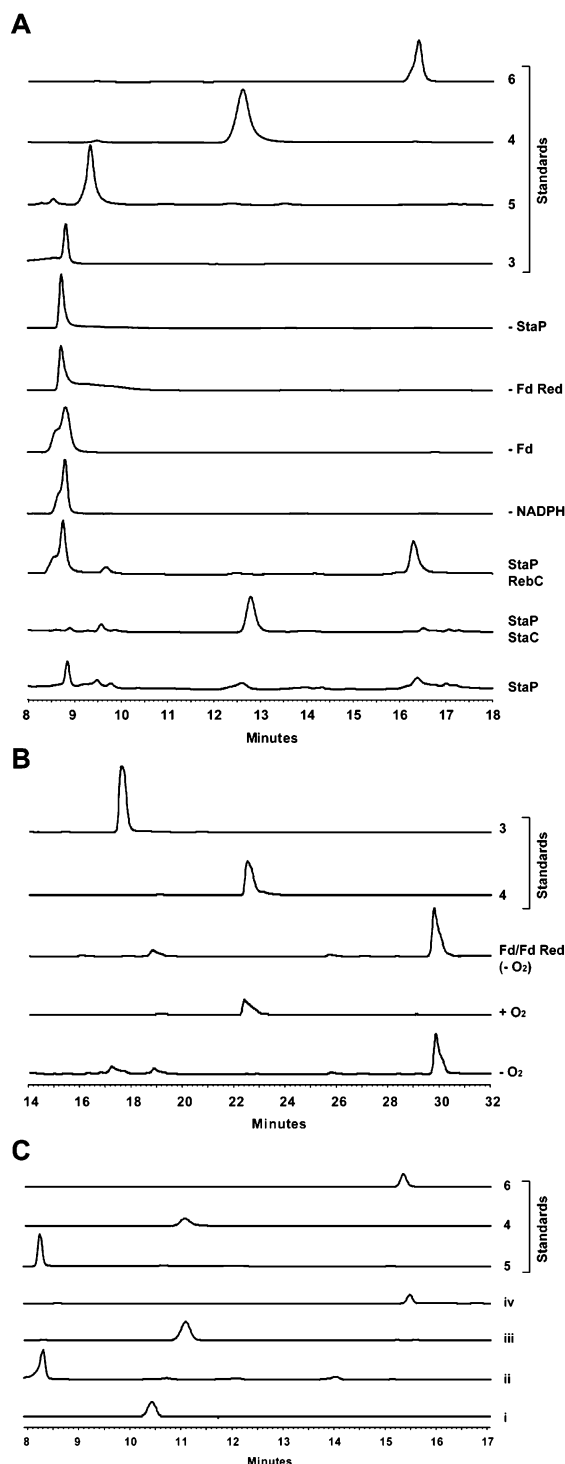


Figure 4. HPLC traces (280 nm) of products formed on incubation of (A) CPA (150 μM) with StaP (1 μM) and StaC (5 μM)—or RebC (5 μM)—in the presence of 75 mM HEPPS, pH 8, 1 $\text{mg}\cdot\text{mL}^{-1}$ BSA, 5 mM NADPH, 20 μM ferredoxin, and 1 μM flavodoxin NADP⁺-reductase for 3 h; (B) in the presence and absence of dioxygen (anaerobic control incorporating only ferredoxin (20 μM) and flavodoxin NADP⁺-reductase (1 μM) in 75 mM HEPPS, pH 8, reveal that new peaks are not CPA-derived); and (C) on incubation of StaP (1 μM) in the presence of 75 mM HEPPS, pH 8, 1 $\text{mg}\cdot\text{mL}^{-1}$ BSA, 5 mM NADPH, 20 μM ferredoxin, and 1 μM flavodoxin NADP⁺-reductase with (i) arcyrinarubin A 9 (100 μM), (ii) 7-hydroxy-K252c 5 (150 μM), (iii) K252c 4 (150 μM), and (iv) arcyrriaflavin A 6. Traces for parts A and C were obtained using a Higgins analytical C18 column (50 mm \times 4.6 mm); part B traces were obtained using a Vydac C18 column (250 mm \times 10 mm). (Identical traces were seen on incubation of each of the aglycones with RebC (5 μM) or StaC (5 μM) in the presence or absence of StaP.)

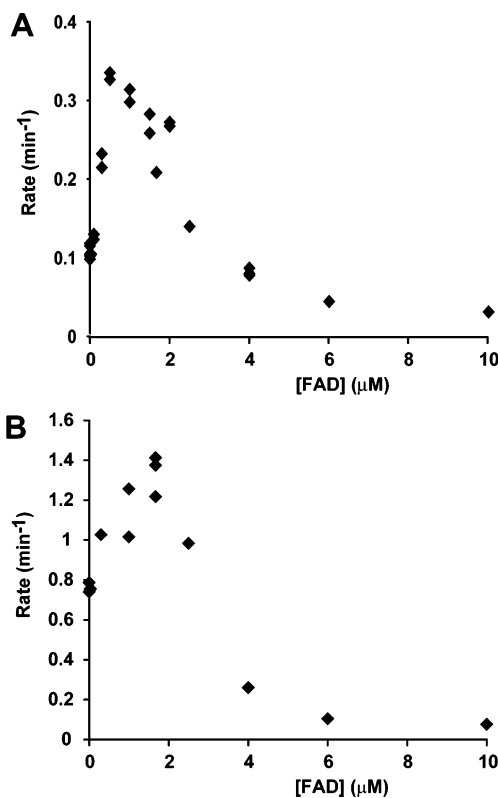


Figure 5. Effect of FAD concentration on observed rate of formation of (A) K252c 4 by StaP (1 μM) and StaC (5 μM) and of (B) arcyrriaflavin A 6 by StaP (1 μM) and RebC (5 μM) from CPA 3 in the presence of 75 mM HEPPS, pH 8, 1 $\text{mg}\cdot\text{mL}^{-1}$ BSA, 5 mM NADPH, 20 μM ferredoxin, and 1 μM flavodoxin NADP⁺-reductase.

Table 1. Steady-State Kinetic Parameters for Turnover of CPA 3 by StaP (1 μM) and StaC (5 μM) or RebC (5 μM) in the Presence of 75 mM HEPPS, pH 8.0, 1 $\text{mg}\cdot\text{mL}^{-1}$ BSA, 5 mM NAD(P)H, 20 μM Ferredoxin, 1 μM Flavodoxin NADP⁺-Reductase, and 0.5 μM FAD (StaP/StaC Assays) or 1.7 μM FAD (StaP/RebC Assays).

	StaP/StaC		StaP/RebC	
	NADH	NADPH	NADH	NADPH
k_{cat} (min^{-1})	3.6 ± 0.9	0.61 ± 0.05	4.1 ± 0.6	1.3 ± 0.1
K_{m} (mM)	76 ± 28	35 ± 9	26 ± 6	26 ± 6
$k_{\text{cat}}/K_{\text{m}}$ ($\text{mM}^{-1} \text{min}^{-1}$)	0.047	0.017	0.15	0.050
K_{i} (mM)	93 ± 35	—	84 ± 19	—

the StaP/StaC and StaP/RebC systems, respectively, were studied under steady-state conditions, and the relevant parameters are given in Table 1. Interestingly, both the StaP/StaC and StaP/RebC systems showed a marked preference for NADH over NADPH as the ultimate reductant in this reaction. For both the StaC and RebC reactions, a 3-fold increase in catalytic efficiency is seen for CPA turnover in the presence of NADH versus that seen in the presence of NADPH. In contrast, the rate of aglycone formation by StaP in isolation does not change if NADH is substituted for NADPH. This overall rate effect therefore seems directly attributable to a StaC/RebC-catalyzed reaction.

In the presence of NADH, the K_{m} values of StaP/StaC and StaP/RebC for CPA differ by approximately 3-fold, but the k_{cat} values are comparable (Table 1). This gives a 3-fold increase in catalytic efficiency in the formation of arcyrriaflavin A 6 by StaP/RebC, relative to the StaP/StaC-mediated formation of K252c 4. Due to substantial substrate inhibition observed in both cases above approximately 70 μM , it is important to note

that the calculated k_{cat} values are never actually realized. The rates of formation of K252c **4** and arcyliaflavin A **6** by StaP in isolation are an order of magnitude lower than those seen for the formation of **4** and **6** in the presence of StaC or RebC, respectively (data not shown). Thus, while StaP is catalytically competent to turn over CPA **3** to the aglycone products **4**, **5**, and **6**, the presence of StaC or RebC give significant boosts in reaction rates as well as providing oxidative control.

Discussion

The extensive oxidative transformations required to generate the rebeccamycin and staurosporine aglycone scaffolds from L-Trp (or 7-Cl-L-Trp) are catalyzed by only four enzymes. The formation of the planar six-ring aglycone core involves a 10- to 14-electron net oxidation of the starting pair of L-Trp (or 7-Cl-L-Trp) molecules. At the crux of this biosynthetic machinery is StaP, which alone can mediate a four- to eight-electron oxidation of its substrate, CPA **3**.

StaP, a cytochrome P450 enzyme, catalyzes an aryl–aryl bond-forming reaction to give a six-ring indolocarbazole scaffold, as well as mediating decarboxylation and oxidation of the putative dicarboxypyrrole moiety. This action presumably requires two to four cycles of net two-electron substrate oxidation at the catalytic heme center. StaP is remarkable, not only due to the extensive oxidation processes it catalyzes, but also because it produces three distinct products, differing in oxidation level. For the production of K252c **4** from CPA **3**, a net four-electron oxidation is required; the generation of arcyliaflavin A **6** from **3** requires an overall eight-electron oxidation. StaP is thus unusual in the apparent lack of oxidative control it possesses over the outcome of its catalytic turnover.

Control of the overall oxidation route is provided by a second enzyme StaC, which imparts the net effect of directing the oxidation level of the pyrrole-derived ring. While StaP in isolation gives three aglycone forms, StaP and StaC turn over CPA to give only a single product, K252c **4**. Similarly, RebC guides the turnover of CPA **3** toward the more highly oxidized maleimide-bearing aglycone, arcyliaflavin A **6**. This *in vitro* behavior of StaP, StaC, and RebC exactly mirrors the previously reported *in vivo* results.^{7,16}

The interaction between StaC and StaP has been investigated (using biochemical pull-down experiments and gel filtration), but no compelling evidence for a stable complex has been observed to date. Although the formation of a weakly associating catalytic complex cannot be ruled out, it seems that these two proteins do not have high affinity for one another.

The ability of StaC and RebC to oxidize NAD(P)H in the presence of FAD suggests that these enzymes may be FAD-dependent monooxygenases, in line with their previous annotation.^{7,16} Given these results, it is interesting to note that StaC does not form a tightly bound complex with FAD, but RebC can be reconstituted up to 0.55 equiv of FAD. The high K_{m} s for FAD seen in NADH oxidation by StaC and RebC further suggest that the FAD/StaC and FAD/RebC complexes may not be strongly associating. The disparity in the FAD-binding capacities of StaC and RebC is intriguing given the high overall homology between these two proteins and the presence of characteristic flavin-binding motifs in both. The relevance of this difference in FAD-binding affinity to the catalytic abilities of these enzymes remains to be determined.

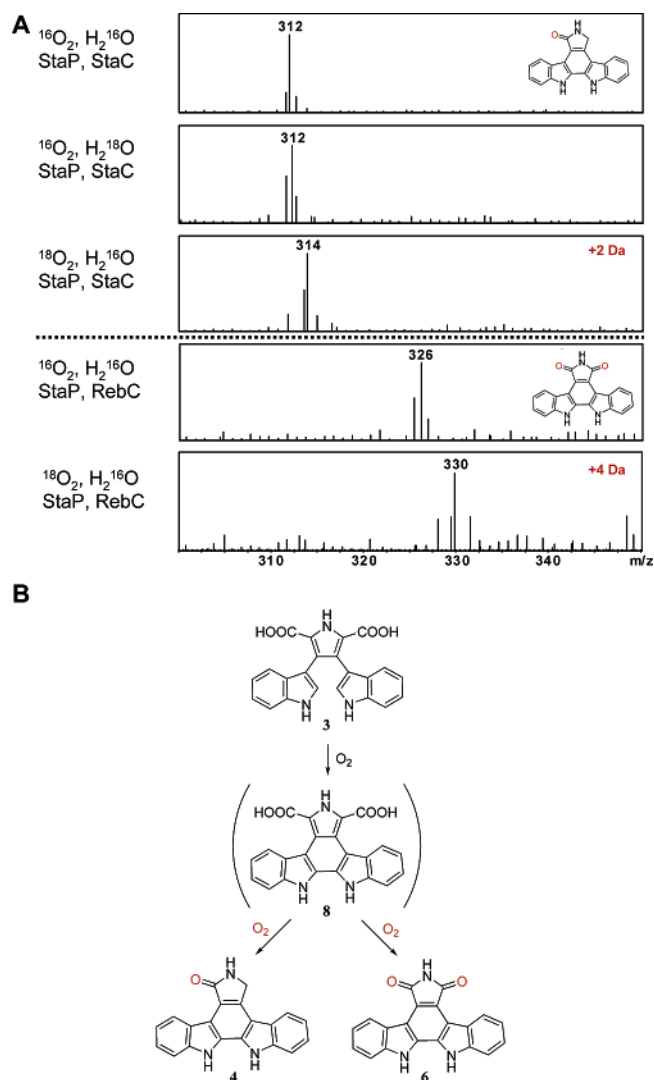
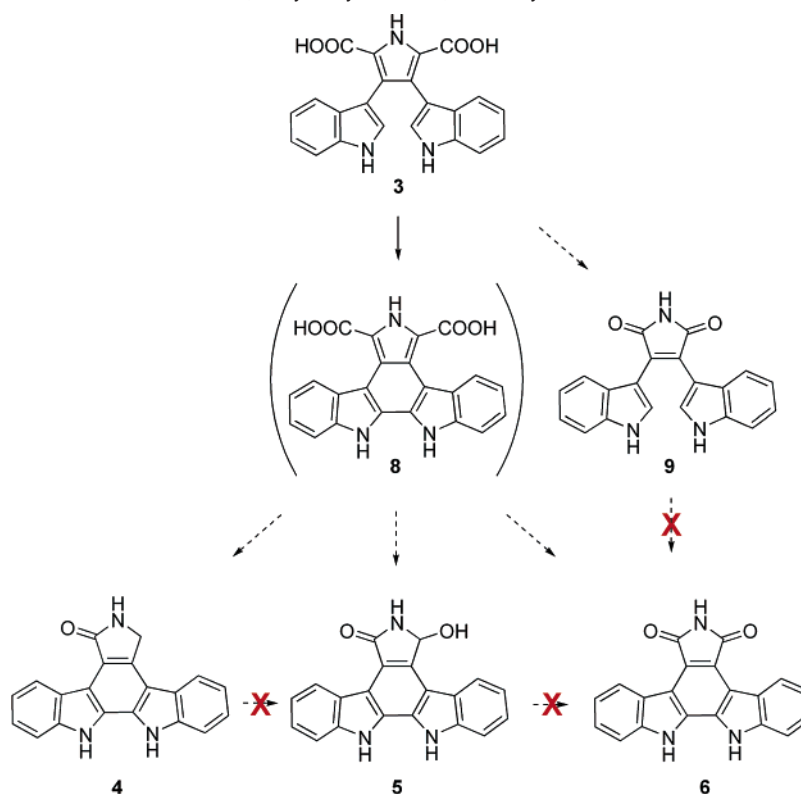


Figure 6. (A) Mass spectra (ES⁺) of products derived from reaction of CPA **3** (150 μM) with StaP (1 μM) and StaC (5 μM) or RebC (5 μM) in the presence of 75 mM HEPES, pH 8, 1 mg·mL⁻¹ BSA, 5 mM NADPH, 20 μM ferredoxin, and 1 μM flavodoxin NADP⁺-reductase, in ¹⁸O-labeled O₂ or water; and (B) biosynthetic route showing incorporation of oxygen atoms from dioxygen.

Exogenous FAD is not required for the catalytic activity of StaC, but does give a 3.6-fold rate enhancement when 0.1 equiv are included in the assay mixture. (A similar effect was observed for RebC, with optimal activity occurring at 0.33 equiv of FAD per RebC molecule.) Since the assays contained in this work utilize flavodoxin NADP⁺-reductase, which contains bound FAD, it is possible that the baseline activity seen in the absence of exogenous FAD derives from competition by StaC or RebC for the reductase-bound flavin.

At higher concentrations of FAD, aglycone formation is significantly inhibited, in the presence or absence of StaC (or RebC). That this inhibition can be partially ameliorated by increasing the concentration of flavodoxin-NADP⁺-reductase suggests that it is due, at least in part, to an interaction between FAD and flavodoxin NADP⁺-reductase. The flavodoxin reductase mechanism involves the transient generation of reduced flavin to facilitate reduction of ferredoxin.²⁹ Excess FAD in solution may compete with reduced flavin in the flavodoxin

(29) Wan, J. T.; Jarrett, J. T. *Arch. Biochem. Biophys.* **2002**, *406*, 116–126.

Scheme 2. Possible Biosynthetic Routes to K252c **4**, 7-Hydroxy-K252c **5**, and Arcyriaflavin A **6**

NADP⁺-reductase active site or may be itself reduced by flavodoxin reductase,³⁰ thus disrupting the redox chain necessary for StaP reactivity. The optimal ratios of 1:10 for FAD:StaC and 1:3 for FAD:RebC observed in this assay almost certainly result from two competing equilibria between FAD/StaC (or FAD/RebC) and FAD/flavodoxin reductase, rather than being a direct indication of the optimal FAD:StaC (or FAD:RebC) binding ratio for catalysis.

The derivation of the oxygen atoms in K252c **4** and arcyriaflavin A **6** had not been previously investigated. Although mechanistic logic would favor the incorporation of oxygen at these positions from dioxygen, this had not been unequivocally proven. In this report, we demonstrate the direct inclusion of oxygen atoms from dioxygen at these positions through the use of ¹⁸O-labeled water and dioxygen. The mass shift of +2 for K252c **4** and +4 for arcyriaflavin A **6** upon incubation with ¹⁸O-labeled dioxygen (relative to incubations with atmospheric dioxygen) indicates that O₂ is the source of the oxygens of the pyrrolinone and maleimide rings of these indolocarbazoles. Due to a high degree of uncoupling between the ferredoxin/flavodoxin NADP⁺-reductase system and StaP, it was not possible to correlate rates of oxygen consumption with product formation. However, based on the stoichiometry of the reaction, it seems likely that four molecules of oxygen are consumed per molecule of arcyriaflavin A **6** formed, and two oxygen molecules utilized for the production of one molecule of K252c **4**.

Our investigations into potential biosynthetic intermediates have allowed us to narrow the possibilities for the overall reaction pathway from CPA **3** to aglycones **4**, **5**, and **6**. One might envisage two overall pathways for the StaP-catalyzed reaction: (a) initial aryl–aryl coupling followed by decarboxy-

lation or (b) oxidative decarboxylation followed by an aryl–aryl coupling step (Scheme 2). The failure of StaP and/or RebC to turn over arcyrarubin A **9** suggests that this is not a biosynthetic intermediate on the pathway to arcyriaflavin A **6**. Hence the likely overall pathway involves initial aryl–aryl coupling to intermediate **8** with subsequent decarboxylation and oxidation. We suggest that StaP is the key aryl–aryl coupling catalyst since StaP is absolutely required for turnover, and StaC and RebC are incapable of reacting with CPA **3**. This oxidative coupling likely proceeds in one-electron steps, following initial reduction of the heme center by reduced ferredoxin and oxygen binding to generate a reactive ferryl-oxo intermediate, according to the typical cytochrome P450 mechanism.³¹

The putative intermediate **8** has not been isolated and is likely quite unstable. Given its highly conjugated nature, decarboxylation may occur spontaneously and, in an aerobic environment, could be accompanied by autooxidation. Such a nonenzymatic decarboxylation/oxidation pathway may go some way to explaining the suite of products formed in the absence of StaC and RebC.

We note that no combination of StaP, StaC, and RebC is able to interconvert any of the three aglycones **4**, **5**, and **6**, suggesting that these aglycones are not on pathway to one another. Thus, it seems that these three aglycones share a common precursor earlier in the biosynthetic pathway and diverge separately from this point. This result is somewhat surprising, since it would seem particularly likely that arcyriaflavin A **6** arises by a two-electron oxidation of 7-hydroxy-K252c **5**, which may in turn be derived from K252c **4**.

The increased rate of product formation observed in the presence of StaC or RebC (relative to that seen with StaP alone)

(30) Uyeda, K.; Rabinowitz, J. C. *J. Biol. Chem.* **1971**, *246*, 3111–3119.

(31) Ullrich, V. *Angew. Chem. Int. Ed.* **1972**, *11*, 701–712.

suggests that these enzymes play physiologically relevant roles in the final steps of aglycone formation, in accord with *in vivo* reports.^{7,16} The most remarkable difference between StaC and RebC is that these two homologous NADH-flavin oxidoreductases catalyze overall flux of the reaction to two distinct products, aglycones **4** and **6**. These products are identical except for a four-electron difference in the oxidation state at one position in the pyrrole-derived ring.

StaC appears to direct the product flux such that the second decarboxylation follows a non-oxidative pathway. By contrast, RebC enables an oxidative pathway (e.g., by providing an hydroxyl radical or cation equivalent) and then presumably mediates a subsequent oxidation to give the maleimide ring of **6**. Given the observed lack of turnover of 7-hydroxy-K252c **5**, this second oxidation (on compound **5**) would have to occur before its irreversible release to solvent. In this manifold, RebC but not StaC would have oxygenase activity itself or function to elicit that reactivity mode from StaP.

It is still unclear, however, as to whether StaC and RebC exert their catalytic effects through direct action on an intermediate or whether they act indirectly via StaP. These enzymes may function directly as FAD monooxygenases, converting the CPA-derived dicarboxypyrrole ring to the pyrrolinone and maleimide rings of the aglycone products, **4** and **6**. It is however surprising that these indolocarbazole-producing actinomycetes would have evolved two parallel (and fundamentally different) systems for catalyzing the same reaction. Alternatively, they may act indirectly, either through feeding electrons into the StaP catalytic center or by exerting some allosteric effect on StaP, rather than effecting substrate oxidation directly.

If StaC and RebC act only through modulating the activity of StaP, the mechanism of this process is still unclear. For example, it has not been possible to discount the option that StaC and RebC simply function to feed electrons into the StaP heme center, which would in turn effect catalytic turnover. However, StaC and RebC cannot substitute for the ferredoxin/flavodoxin NADP⁺-reductase redox system, which is absolutely required for catalysis, and hence it is difficult to rationalize an obligate role for two redox feeder systems for the heme iron center. Furthermore, there are no known redox partners bearing FAD that directly interact with cytochrome P450 enzymes. Rather, iron-sulfur clusters (e.g., ferredoxins) and FMN (e.g., cytochrome P450 reductases and flavodoxins) are preferred as the immediate electron donors for the P450 heme center.²⁸

Either way, however, it seems that the increased specificity and efficiency of aglycone formation in the presence of StaC and RebC are FAD- and NADH-dependent effects. In the presence of both StaC and RebC (but not in their absence), an increase in the rate of aglycone formation is observed in the presence of NADH, relative to that seen with NADPH. NADH is the preferred reductant for FAD oxidation by StaC, with a 13-fold enhancement in $k_{\text{cat}}/K_{\text{m}}$ relative to that seen with NADPH; flavodoxin- NADP⁺-reductase shows the inverse preference, with a 5-fold greater catalytic efficiency with NADPH versus NADH.³² Therefore, the 3-fold $k_{\text{cat}}/K_{\text{m}}$ improvement for the StaP/StaC-mediated formation of **4** and the StaP/

RebC-mediated production of **6** in the presence of NADH appears to be due to a direct interaction between NADH and StaC or RebC. In addition, the dependence of the reaction rate on FAD concentration suggests the involvement of StaC. A 3.5-fold increase in catalytic efficiency for the StaP/StaC reaction is observed when the FAD concentration is increased from 0 to 0.5 μM , but no rate enhancement is seen in the absence of StaC or RebC. Taken together, these results suggest that the enhanced reaction rates seen in the presence of StaC and RebC are FAD- and NADH-dependent effects that involve StaC or RebC in a catalytic manner.

Since StaC and RebC are not catalytically competent to turn over CPA **3**, it seems likely that the physiological role of StaP is to form a key intermediate through mediating initial aryl–aryl coupling. Decarboxylation of the highly conjugated six-ring scaffold **8** would follow, perhaps via a nonenzymatic process, with StaP, StaC, or RebC mediating aglycone formation from this intermediate stage.

In summary, this work demonstrates reconstitution of the full staurosporine and rebeccamycin biosynthetic pathways from L-Trp (or 7-Cl-L-Trp) to the staurosporine aglycone K252c **4** and the rebeccamycin aglycone 1,11-dichloroarcyriaflavin A **7**. The results described herein specifically address the biosynthetic route from CPA **3** to the staurosporine- and rebeccamycin-related aglycones, K252c **4**, 7-hydroxy-K252c **5**, and arcyriaflavin A **6**. We postulate that the overall reaction is initiated by StaP-mediated aryl–aryl coupling of chromopyrrolic acid to give a dicarboxylated six-ring intermediate **8** (Scheme 2). Enzyme-mediated aryl–aryl coupling steps are poorly understood processes. The robust aryl–aryl coupling reaction catalyzed by StaP, as well as the subsequent oxidative decarboxylation to form the rebeccamycin and staurosporine aglycone scaffolds, lend the StaP/StaC enzyme system much appeal. The significant oxidative changes mediated by StaP are particularly striking given that these transformations require only a single enzyme. Furthermore, the catalytic roles of StaC and RebC in enhancing rates of aglycone formation and controlling the oxidative outcome of the reaction are intriguing. This work represents a starting point for future mechanistic studies into the enzymes responsible for this complex and intriguing catalytic cycle.

Acknowledgment. We thank Prof. Rowena Matthews for provision of a flavodoxin NADP⁺-reductase construct and Prof. Robert S. Phillips for providing an authentic sample of 7-Cl-L-Trp. We thank Dr. Wendy L. Kelly for helpful discussions. This work was supported by National Institutes of Health Grant GM020011.

Supporting Information Available: Sequences for *staC* and *staP* from *S. longisporoflavus* (DSM 10189) and complete ref 20. This information is available free of charge via the Internet at <http://pubs.acs.org>.

JA063898M

- (32) Leadbeater, C.; McIver, L.; Campopiano, D. J.; Webster, S. P.; Baxter, R. L.; Kelly, S. M.; Price, N. C.; Lysek, D. A.; Noble, M. A.; Chapman, S. K.; Munro, A. W. *Biochem. J.* **2000**, *352*, 257–266.